Taylor & Francis
Taylor & Francis Group

Journal of Computational and Graphical Statistics

ISSN: 1061-8600 (Print) 1537-2715 (Online) Journal homepage: https://www.tandfonline.com/loi/ucgs20

A Bayesian Time-Varying Coefficient Model for Multi-Type Recurrent Events

Yi Liu & Feng Guo

To cite this article: Yi Liu & Feng Guo (2019): A Bayesian Time-Varying Coefficient Model for Multi-Type Recurrent Events, Journal of Computational and Graphical Statistics, DOI: 10.1080/10618600.2019.1686988

To link to this article: https://doi.org/10.1080/10618600.2019.1686988

A Bayesian Time-Varying Coefficient Model for Multi-Type Recurrent Events

Yi Liu, Feng Guo*

Department of Statistics, Virginia Tech

Department of Statistics, Virginia Tech, Virginia Tech Transportation Institute

*Corresponding author: Feng Guo feng.guo@vt.edu

Abstract

This paper proposes a Bayesian time-varying coefficient model to evaluate the temporal profile of intensity for multi-type recurrent events. The model obtains smooth estimates for both time-varying coefficients and the baseline intensity using Bayesian penalized splines. One major challenge in Bayesian penalized splines is that the smoothness of a spline fit is sensitive to the subjective choice of hyperparameters. We establish a procedure to objectively determine the hyperparameters through robust prior specification. To effectively update the high-dimensional spline parameters, we develop a Markov chain Monte Carlo procedure based on the Metropolis-adjusted Langevin algorithms. A joint sampling scheme is used to achieve better convergence and mixing properties. A simulation study confirms satisfactory model performance in estimating time-varying coefficients under different curvature and event rate scenarios. Application to a commercial truck driver naturalistic driving data reveals that drivers with 7-hours-or-less sleep time have a significantly higher safety-critical event intensity after 8 hours of driving and the intensity remains high after taking a break. The findings provide crucial information for the truck driver hours-of-service regulation and fatigue management. The proposed model provides a flexible and robust tool to evaluate the temporal profile of intensity for multi-type recurrent events.

Keywords: multivariate frailty, penalized splines, Metropolis-adjusted Langevin algorithms, truck driving safety, naturalistic driving study

1 Introduction

Recurrent events can be observed in medical and epidemiological studies in which individuals experience events of interest repeatedly over a period of time.

It is common for individuals to be at risk for more than one type of events. For example, patients in skin cancer trials are at risk of recurrence of both basal cell epithelioma and squamous cell carcinoma tumors (Abu-Libdeh et al. 1990), and recurrent asthma exacerbations for respiratory studies can be classified by sputum cell counts as eosinophilic or non-eosinophilic (Jayaram et al. 2006). One interesting aspect of multi-type recurrent event modeling is to evaluate how the intensity varies over a period of time as well as how the profile is affected by other factors. Limited research has been conducted to address this issue and the purpose of this study is to develop a general and flexible method for characterizing the temporal patterns of multi-type recurrent events.

Multi-type recurrent event analysis typically includes marginal models based on estimating functions (e.g., Ng and Cook 1999; Cai and Schaubel 2004) and joint models based on multivariate frailties (e.g., Abu-Libdeh et al. 1990; Chen et al. 2005). Methods using estimating functions are constructed to directly describe marginal means and treat the dependence structure of events as nuisance parameters. In contrast, joint models use multivariate frailties to characterize the heterogeneity and correlation among events, and allow both marginal and conditional inferences.

The temporal profile of the baseline intensity could be of interest in many studies. One common approach for baseline modeling is to use a piecewise-constant intensity form (e.g., Chen et al. 2005; Chen and Cook 2009). Li et al. (2017) and Li et al. (2018) used change-point models based on piecewise-constant intensity functions to detect the time of change in driving risks for novice teenage drivers. However, baseline modeling that relies on piecewise-constant forms requires accurate specification of the number and locations of pieces (Friedman 1982). An alternative approach is based on nonparametric baseline assumptions and yields an estimator similar to the Nelson-Aalen estimator (Aalen 1978) from survival analysis. The estimator is robust with respect to assumptions but might be unstable in regions of sparse data (Cai and Betensky 2003).

There are situations where a smooth intensity form is desired. For example, it is beneficial to estimate covariate effects for interval-censored data (Cai et al. 2002). Nielsen and Dean (2005) employed regression splines to model recurrent events, though there is no guarantee of monotonicity for the cumulative intensity estimate for small sample size situations. The development of a more general and flexible method is needed for smooth estimation of baseline intensity.

The effect of a covariate can vary over time for recurrent events and could be of primary interest. For example, total sleep time the night before driving is a critical risk factor affecting driver fatigue, and its impact on driving performance is likely to change over a long shift due to increasing fatigue over time (Hanowski et al. 2007). In the Commercial Truck Driver Naturalistic Driving Study (see Section 5 for details), the research question is how driving performance varies over time and the impact of sleep time on its temporal profile. Varying coefficient models for longitudinal data include kernel-based methods (e.g., Carroll et al. 1998; Fan and Zhang 1999; Cai et al. 2000) and spline-based methods (e.g., Hastie and Tibshirani 1993; Huang et al. 2002). Kernel estimators are constructed through a weighted mean of the nearby observations and have great intuitive appeal. However, the kernel weights are asymmetric at the boundaries of the predictor space and could cause substantial bias for the estimate (Hastie and Loader 1993). Spline estimators are based on linear combinations of piecewise polynomial functions and are a straightforward extension of linear regression models. The computations are relatively fast and can be easily implemented (Eilers and Marx 1996). Although research has been conducted on varying coefficients for recurrent event data (Amorim et al. 2008; Sun et al. 2011; Yu et al. 2013; Lin et al. 2017), there is limited work on multi-type recurrent events that simultaneously incorporates baseline modeling, time-varying coefficient estimation while also accounting for the dependence structure between event types.

To assess the time-varying patterns for multi-type recurrent events, this paper proposes a Bayesian joint model with time-varying coefficients. The joint model is based on multivariate log-normal frailties to characterize the heterogeneity and correlation among different event types. The proposed model uses Bayesian penalized splines (Lang and Brezger 2004) to achieve smooth estimates for both time-varying coefficients and the baseline intensity. The cumulative intensity in the posterior is then approximated by numerical integration based on the trapezoid method (Kauermann 2005). In Bayesian penalized splines, the smoothness of a spline fit depends substantially on the subjective choice of hyperparameters (Brezger and Lang 2006). However, re-fitting the model with a number of choices can be computationally demanding. To address this, we employ a robust prior specification (Jullion and Lambert 2007) to achieve an objective fitting procedure. One challenge in using Markov chain Monte Carlo methods for posterior inference is sampling from the high-dimensional distribution of spline parameters. This work uses Metropolis-adjusted Langevin algorithms (MALA; Roberts and Tweedie 1996), a class of Metropolis-Hastings algorithms whose proposals are based on the gradient of the target density. Another concern in sampling spline parameters is that the MALA proposal strongly depends on a roughness penalty parameter introduced by Bayesian penalized splines. Updating these two parameters separately could lead to convergence issues. We integrate MALA algorithms into a joint sampling scheme (Knorr-Held and Rue 2002) for better convergence and mixing properties. This proposed approach provides a general approach that can be directly implemented while still providing smooth estimates for features of multi-type recurrent event data.

The naturalistic driving studies (NDS) is a primary source for evaluating traffic safety, crash risk, and driver behavior (Guo et al. 2017; Dingus et al. 2016; Klauer et al. 2014; Guo et al. 2013; Guo and Fang 2013). A large scale NDS collects continuous driving and driver behavior information through advanced in-vehicle instrumentation with multiple cameras, three-dimensional

accelerometer, and radar *et al* (Dingus et al. 2015). The novel NDS data also bring challenges in statistical modeling and various methods have been used in analyzing NDS, e.g.,epidemiology, regression, and causal inference (Guo 2019). The continuously collected high resolution data make it possible to identify multiply types of safety events, e.g., crashes, near-crashes, crash-relevant conflicts, and unintentional lane deviations. Many of such events could occur multiple times for a driver and recurrent event models have been used to assess the impact of crashes on driving behavior, risk change point of novice teenage driver, and truck driver performance over a long driving shift (Chen and Guo 2016; Li et al. 2017, 2018; Liu et al. 2019).

This paper uses data from the Commercial Truck Driver Naturalistic Driving Study (Blanco et al. 2011) as an example for application. The Commercial Truck Driver NDS is a large-scale naturalistic driving that collected data from approximate 100 commercial truck drivers. The proposed approach was applied to evaluate how driving performance and driving risk changes over time and to compare this temporal profile by different total sleep time prior to on-duty shift driving.

The remainder of the paper is organized as follows. Section 2 introduces a Bayesian joint model with time-varying coefficients. Section 3 describes the joint posterior sampling scheme, in which the MALA algorithm is integrated for sampling from the high-dimensional distribution of spline parameters. A simulation study is presented in Section 4. Section 5 applies the proposed method to data from the Commercial Truck Driver Naturalistic Driving Study. Section 6 provides a summary and discussion.

2 Model

The proposed approach is a joint model based on multivariate log-normal frailties with time-varying coefficients. Bayesian penalized splines are used to model both time-varying coefficients and the baseline intensity. To address the issue that

subjective choices of hyperparameters control the smoothness of a spline fit, a robust prior specification approach is adopted to achieve an objective fitting procedure.

Let $1 \le i \le I$ be the index of event processes and $1 \le j \le J$ be the index of event types. Let $N_{ij}(t)$ denote the number of type *j* events that occurred over $[0,t]$ for process *i*. The multivariate event process is $\{\boldsymbol{N}_i(t), t \ge 0\}$, where $\boldsymbol{N}_i(t) = (N_{i1}(t), \ldots, N_{iJ}(t))'$. Let $\boldsymbol{x}_i$ denote a vector of covariates with constant coefficients, and $\boldsymbol{z}_i = (z_{i1}, \ldots, z_{iq})'$ denote covariates with time-varying coefficients. We use $\boldsymbol{H}_i(t) = \{\boldsymbol{N}_i(s), 0 \le s < t, \boldsymbol{x}_i, \boldsymbol{z}_i\}$ to represent the process history at time *t*, which includes the times and types of events that occurred over $[0,t)$ as well as their covariate values. Let $\Delta N_{ij}(t)$ denote the number of type *j* events in $[t, t+\Delta t)$. Conditional on a random effect b_{ij}, the intensity function for type *j* events is (Cook and Lawless 2007)

$$\lambda_{ij}(t \mid \boldsymbol{H}_i(t), b_{ij}) = \lim_{\Delta t \downarrow 0} \frac{P(\Delta N_{ij}(t) = 1 \mid \boldsymbol{H}_i(t), b_{ij})}{\Delta t}. \quad (1)$$

We assume that $\{N_{ij}(t), t \ge 0\} \mid \boldsymbol{x}_i, \boldsymbol{z}_i, b_{ij}$ is an independent Poisson process with the conditional intensity formulated as

$$\lambda_{ij}(t \mid \boldsymbol{x}_i, \boldsymbol{z}_i, b_{ij}) = \exp\{\boldsymbol{x}_i' \boldsymbol{\alpha}_j + \beta_{0j}(t) + z_{i1}\beta_{1j}(t) + \cdots + z_{iq}\beta_{qj}(t) + b_{ij}\}. \quad (2)$$

$\boldsymbol{\alpha}_j$ is a vector of unknown regression coefficients and $\boldsymbol{x}_i' \boldsymbol{\alpha}_j$ represents the linear component of the log intensity. $\beta_{0j}(t), \beta_{1j}(t) \ldots, \beta_{qj}(t)$ are unknown smooth functions: $\beta_{0j}(t)$ is the log baseline intensity and the rest are time-varying coefficients of the covariates in $\boldsymbol{z}_i$. We assume that $\boldsymbol{b}_i = (b_{i1}, \ldots, b_{iJ})'$ is an independent and identical normal variate with density $p(\boldsymbol{b}_i \mid \boldsymbol{\Sigma}) = N_J(\boldsymbol{0}, \boldsymbol{\Sigma})$. The variances in $\boldsymbol{\Sigma}$ characterize extra-Poisson variation and association of event counts from each process, and the covariances characterize association between different event types. This frailty distribution allows separate parameters

for variances and covariances, thus providing flexibility for the dependence structure among event types.

To model the baseline intensity and time-varying coefficients, we assume that $\beta_{lj}(t), 0 \le l \le q$, can be approximated by polynomial splines of degree v with equally spaced knots $t_{\min} = \zeta_{l0} < \zeta_{l1} < \cdots < \zeta_{l,k_l} = t_{\max}$ over the domain of time t. Let $B_{lk}(t)$ denote the value at t of the kth B-spline, and $\boldsymbol{B}_{\boldsymbol{l}}(t) = (B_{l1}(t), \ldots, B_{l,K_l}(t))'$ denote $K_l = k_l + v$ B-spline basis functions. The parameterization used for splines is

$$\beta_{lj}(t) = \sum_{k=1}^{K_l} B_{lk}(t)\beta_{klj} = \boldsymbol{B}_{\boldsymbol{l}}'(t)\boldsymbol{\beta}_{\boldsymbol{lj}}. \qquad (3)$$

$\boldsymbol{\beta}_{\boldsymbol{lj}} = (\beta_{1lj}, \ldots, \beta_{K_l,lj})'$ is a vector of unknown regression coefficients for splines. To ensure enough flexibility for the fit, a moderately large number of knots should be chosen. However, this commonly leads to severe overfitting. Eilers and Marx (1996) proposed a frequentist solution based on a roughness penalty. Let Δ denote the difference operator such that the first order difference of β_{klj} is $\Delta\beta_{klj} = \beta_{klj} - \beta_{k-1,lj}$, the second order difference is $\Delta^2\beta_{klj} = \beta_{klj} - 2\beta_{k-1,lj} + \beta_{k-2,lj}$, etc. In general, a roughness penalty based on the rth order difference

$$\text{pen}(\lambda_{ij}) = \frac{\lambda_{lj}}{2} \sum_{k=r+1}^{K_l} (\Delta^r \beta_{klj})^2 \qquad (4)$$

is subtracted from the log likelihood and parameters are estimated via maximizing the resulting penalized function. The smoothness of a spline fit is controlled by the smoothing parameter λ_{lj}: by increasing λ_{lj}, the amount of roughness penalty increases and the smoothness is tuned accordingly. The smoothing parameter has to be selected by cross-validation or optimizing some information criterion. In our setting, the computational cost grows as the number of time-varying coefficients increases. The procedure could fail in practice since no optimal solution for λ_{lj} can be found (Lang and Brezger 2004). Another

drawback is that the frequentist approach assumes λ_{lj} to be a known fixed quantity, and therefore underestimates the variances for spline parameters in $\boldsymbol{\beta}_{lj}$, yielding narrow confidence intervals for $\beta_{lj}(t)$.

The model described in this paper uses a Bayesian approach for penalized splines by replacing the roughness penalty in (4) with a random walk of the same order. For example, the first order difference $\Delta\beta_{klj}$ corresponds to a first order random walk $\beta_{klj} = \beta_{k-1,lj} + \epsilon_{klj}$ with $\epsilon_{klj} \sim N(0, 1/\tau_{lj})$. In general, we assume that, for $r+1 \le k \le K_l$, $\Delta^r \beta_{klj}$ follows an independent and identical normal distribution $N(0, 1/\tau_{lj})$. Let $\boldsymbol{D}_l$ be a matrix such that $\boldsymbol{D}_l \boldsymbol{\beta}_{lj} = (\Delta^r \beta_{r+1,lj}, \ldots, \Delta^r \beta_{K_l,lj})'$, then the prior for $\boldsymbol{\beta}_{lj}$ can be equivalently written as

$$p(\boldsymbol{\beta}_{lj} \mid \tau_{lj}) \propto \tau_{lj}^{\rho(\boldsymbol{D}_l)/2} \exp\left\{-\frac{\tau_{lj}}{2} \boldsymbol{\beta}_{lj}' (\boldsymbol{D}_l' \boldsymbol{D}_l) \boldsymbol{\beta}_{lj}\right\}. \qquad (5)$$

The prior is a multivariate normal distribution with mean $\mathbf{0}$ and precision matrix $\tau_{lj}(\boldsymbol{D}_l' \boldsymbol{D}_l)$, where $\boldsymbol{D}_l' \boldsymbol{D}_l$ is rank deficient with rank $\rho(\boldsymbol{D}_l) = K_l - r$. The unknown τ_{lj}, often called the roughness penalty parameter, plays the role of λ_{lj} as in the frequentist approach. We assign a conjugate Gamma prior $\mathrm{Ga}(a, b)$ to τ_{lj}, i.e.,

$$p(\tau_{lj}) = \frac{b^a}{\Gamma(a)} \tau_{lj}^{a-1} \exp(-b\tau_{lj}). \quad (6)$$

The hyperparameters a and b need to be small to yield a non-informative prior, for example, a = 1 and b = 0.005, or $a = b = 0.001$.

It should be noted that the smoothness of a spline fit depends considerably on the choice of a and b (Brezger and Lang 2006). Their connection can be demonstrated by integrating τ_{lj} from the joint posterior. Let $\boldsymbol{\Omega}$ denote all the parameters in the model, and $\boldsymbol{\Omega}^{-lj}$ denote all the parameters excluding $(\boldsymbol{\beta}_{lj}, \tau_{lj})$. Let $L(\boldsymbol{\Omega})$ be the likelihood and $p(\boldsymbol{\Omega}^{-lj})$ be the joint prior for parameters in $\boldsymbol{\Omega}^{-lj}$,

then the joint posterior is $L(\boldsymbol{\Omega})\,p(\boldsymbol{\Omega}^{-lj})\,p(\boldsymbol{\beta_{lj}} \mid \tau_{lj})\,p(\tau_{lj})$. By integrating τ_{lj} out, we obtain the log marginal posterior

$$\log \int L(\boldsymbol{\Omega})\,p(\boldsymbol{\Omega}^{-lj})\,p(\boldsymbol{\beta_{lj}} \mid \tau_{lj})\,p(\tau_{lj})\,\mathrm{d}\tau_{lj} = \log L(\boldsymbol{\Omega}) + \log p(\boldsymbol{\Omega}^{-lj}) - \mathrm{pen}(a,b), \quad (7)$$

where

$$\mathrm{pen}(a,b) = [a + \rho(\boldsymbol{D}_l)/2]\log\Big[1 + \frac{1}{2b}\boldsymbol{\beta_{lj}}'(\boldsymbol{D}_l'\boldsymbol{D}_l)\boldsymbol{\beta_{lj}}\Big]. \quad (8)$$

The marginal posterior corresponds to a frequentist penalized function with a roughness penalty, which differs from that defined in (4). The role of *b* is therefore crucial: as *b* approaching 0, the penalty (8) will become extremely large, which eventually forces a linear fit (for *r* = 2) or a quadratic fit (for *r* = 3). The influence of *a* is limited. Jullion and Lambert (2007) also noted that in practice, no relevant information about *a* could be obtained from the posterior. To address the control of *b* over the fit, we adopt a robust specification by assigning hyperpriors in a higher level of the hierarchy. The hyperparameter *b* is reparameterized as $b = a\delta_{lj}$, while δ_{lj} is assigned to a Gamma hyperprior, $\mathrm{Ga}(a_\delta, b_\delta)$, that is,

$$p(\tau_{lj} \mid \delta_{lj}) \propto \delta_{lj}^{a}\,\tau_{lj}^{a-1}\exp(-a\delta_{lj}\tau_{lj}), \quad (9)$$

$$p(\delta_{lj}) \propto \delta_{lj}^{a_\delta - 1}\exp(-b_\delta\delta_{lj}). \quad (10)$$

We choose small values (e.g., 0.001) for a_δ and b_δ to yield a non-informative hyperprior.

3 Posterior Inference Using MALA Algorithms

This section describes the joint posterior and the MALA algorithms for sampling high-dimensional spline parameters in $\boldsymbol{\beta_{lj}}$. Since $\boldsymbol{\beta_{lj}}$ and τ_{lj} have a strong dependence, updating them separately could cause convergence issues in

MCMC. We therefore integrate MALA algorithms in a joint sampling scheme for block updating $(\boldsymbol{\beta}_{lj}, \tau_{lj})$.

3.1 The posterior

Let t_{ijk} denote the time to the kth type j event for process i. Suppose $n_{ij}(\geq 0)$ events of type j are observed at times $0 < t_{ij1} < \ldots < t_{ij,n_{ij}}$ before censoring time c_i. Let $\boldsymbol{D}_i^{\text{obs}}$ denote the observed data for process i, which includes the times and types of events, the censoring time, and the covariate values. The conditional likelihood for process i is

$$L(\boldsymbol{\alpha}_j, \boldsymbol{\beta}_{lj}, 1 \leq j \leq J, 0 \leq l \leq q; \boldsymbol{b}_i, \boldsymbol{D}_i^{\text{obs}}) = \prod_{j=1}^{J} \left\{ \prod_{k=1}^{n_{ij}} \lambda_{ij}(t_{ijk} \mid \boldsymbol{x}_i, \boldsymbol{z}_i, b_{ij}) \exp\left(-\Lambda_{ij}(c_i)\right) \right\}, \quad (11)$$

where $\Lambda_{ij}(c_i) = \int_0^{c_i} \lambda_{ij}(t \mid \boldsymbol{x}_i, \boldsymbol{z}_i, b_{ij}) \mathrm{d}t$. Since there is no analytic solution to $\Lambda_{ij}(c_i)$, we use the trapezoid method for numerical integration (Kauermann 2005). Consider a grid of points $0 = s_0 < s_1 < \cdots < s_m = t_{\max}$ over the domain of time. For process i, define $m_i = \min\{k : s_k \geq c_i\}$. We approximate $\Lambda_{ij}(c_i)$ by a polygon going through points $(s_k, \lambda_{ij}(s_k))$, where $0 \leq k \leq m_i - 1$, and $\lambda_{ij}(s_k) = \lambda_{ij}(s_k \mid \boldsymbol{x}_i, \boldsymbol{z}_i, b_{ij})$. The approximation yields

$$\begin{aligned} \Lambda_{ij}(c_i) &\approx (c_i - s_{m_i-1}) \frac{\lambda_{ij}(s_{m_i}) + \lambda_{ij}(s_{m_i-1})}{2} + I(m_i \geq 2) \sum_{k=1}^{m_i-1} (s_k - s_{k-1}) \frac{\lambda_{ij}(s_k) + \lambda_{ij}(s_{k-1})}{2} \\ &= \frac{1}{2} \min(c_i, s_1) \lambda_{ij}(s_0) + \frac{1}{2} \sum_{k=1}^{m_i} \left[\min(c_i, s_{k+1}) - \min(c_i, s_{k-1}) \right] \lambda_{ij}(s_k), \end{aligned} \quad (12)$$

where $I(\cdot)$ is the indicator function.

Let $\boldsymbol{\Omega} = (\boldsymbol{\Sigma}, \boldsymbol{\alpha}_j, \boldsymbol{\beta}_{lj}, \tau_{lj}, \delta_{lj}, 1 \leq j \leq J, 0 \leq l \leq q)$, the joint posterior is given by

$$p(\boldsymbol{\Omega} \mid \boldsymbol{D}_i^{\text{obs}}, 1 \le i \le I)$$

$$\propto \prod_{i=1}^{I} L(\boldsymbol{\alpha}_j, \boldsymbol{\beta}_{lj}, 1 \le j \le J, 0 \le l \le q; \boldsymbol{b}_i, \boldsymbol{D}_i^{\text{obs}})\, p(\boldsymbol{b}_i \mid \boldsymbol{\Sigma}) \quad (13)$$

$$\prod_{j=1}^{J} \prod_{l=0}^{q} p(\boldsymbol{\beta}_{lj} \mid \tau_{lj})\, p(\tau_{lj} \mid \delta_{lj})\, p(\delta_{lj}) \cdot \prod_{j=1}^{J} p(\boldsymbol{\alpha}_j) \cdot p(\boldsymbol{\Sigma}),$$

where $p(\boldsymbol{b}_i \mid \boldsymbol{\Sigma}) = N_J(\boldsymbol{0}, \boldsymbol{\Sigma})$; $p(\boldsymbol{\beta}_{lj} \mid \tau_{lj})$, $p(\tau_{lj} \mid \delta_{lj})$, and $p(\delta_{lj})$ are given in (5), (9) and (10). Since there is no restriction on $\boldsymbol{\alpha}_j$, we assign normal priors $N(0, 10^3)$ to the parameters in $\boldsymbol{\alpha}_j$. A standard choice for prior $p(\boldsymbol{\Sigma})$ is the conjugate inverse-Wishart distribution. However, the prior is restrictive since a single degree of freedom parameter controls dependence between all the elements in $\boldsymbol{\Sigma}$. This paper uses a flexible approach based on the Cholesky decompositions. Decomposition has been studied extensively for modeling the covariance matrix of longitudinal data (e.g., Pourahmadi 1999; Chen and Dunson 2003), and has been used for recurrent event data as well (Chen et al. 2005; Lin et al. 2017). Through decomposition, we are able to achieve an unconstrained reparameterization of $\boldsymbol{\Sigma}$ while retaining its positive-definiteness property. Given that $\boldsymbol{\Sigma}$ is real-valued, symmetric, and positive definite, the Cholesky decomposition of $\boldsymbol{\Sigma}$ is unique with form $\boldsymbol{\Sigma} = \boldsymbol{\Phi}\boldsymbol{\Phi}'$, where $\boldsymbol{\Phi}$ is a real-valued lower triangular matrix with positive diagonal entries (e.g., Golub and Van Loan 1983, p. 88). For computational convenience, we use a reparameterization: $\boldsymbol{b}_i = \boldsymbol{\Phi}\boldsymbol{u}_i$, with $\boldsymbol{u}_i \sim N_J(\boldsymbol{0}, \boldsymbol{I})$. Normal priors $N(0, 10^3)$ are then assigned to the below-diagonal entries in $\boldsymbol{\Phi}$, while truncated priors $N(0, 10^3)$ with a positive truncation range are assigned to the diagonal entries.

3.2 Sampling spline parameters

Sampling from the high-dimensional distribution of spline parameters is not trivial. In normal regression models, Lang and Brezger (2004) used a sampling technique based on numerical decompositions for band matrices (Rue 2001). In generalized additive models, Brezger and Lang (2006) developed sampling schemes based on iteratively weighted least squares originally used for

estimating generalized linear models (Fahrmeir and Lang 2001). In the recurrent event setting discussed here, we sample spline parameters using MALA algorithms, a class of Metropolis-Hastings algorithms whose proposals exploit local properties of the target density. Compared to random-walk Metropolis algorithms, MALA provides faster convergence speed and better mixing chains while remaining simple to implement. Lambert and Eilers (2005) used the algorithm in a discrete life-table approach for survival analysis. However, as demonstrated later, MALA proposals depend considerably on the value of roughness penalty parameters. Separately updating spline and roughness penalty parameters could cause convergence issues. To remedy the issue, we integrate MALA proposals in a joint sampling scheme for block updating spline and roughness penalty parameters.

Let $\pi(\boldsymbol{\beta}_{lj})$ denote the full conditional for $\boldsymbol{\beta}_{lj}$, that is, $\pi(\boldsymbol{\beta}_{lj}) \propto L(\boldsymbol{\beta}_{lj})\, p(\boldsymbol{\beta}_{lj} \mid \tau_{lj})$, where $L(\boldsymbol{\beta}_{lj})$ is a product of likelihoods in (11) concerning $\boldsymbol{\beta}_{lj}$ only. Let ∇ denote the gradient operator, and $\boldsymbol{\beta}_{lj}^{\,t}$ denote the state of the chain at iteration *t*. The candidate $\boldsymbol{\beta}_{lj}^{\,*}$ for the next state is generated from a multivariate normal proposal

$$q(\boldsymbol{\beta}_{lj}^{\,t}, \boldsymbol{\beta}_{lj}^{\,*}) \sim N_{K_l}\left(\boldsymbol{\beta}_{lj}^{\,t} + \frac{h}{2}\boldsymbol{M}\nabla \log \pi(\boldsymbol{\beta}_{lj}^{\,t}), h\boldsymbol{M}\right), \qquad (14)$$

and the candidate is accepted with probability

$$\alpha(\boldsymbol{\beta}_{lj}^{\,t}, \boldsymbol{\beta}_{lj}^{\,*}) = \frac{L(\boldsymbol{\beta}_{lj}^{\,*})\, p(\boldsymbol{\beta}_{lj}^{\,*} \mid \tau_{lj}^{t})}{L(\boldsymbol{\beta}_{lj}^{\,t})\, p(\boldsymbol{\beta}_{lj}^{\,t} \mid \tau_{lj}^{t})} \cdot \frac{q(\boldsymbol{\beta}_{lj}^{\,*}, \boldsymbol{\beta}_{lj}^{\,t})}{q(\boldsymbol{\beta}_{lj}^{\,t}, \boldsymbol{\beta}_{lj}^{\,*})}. \quad (15)$$

The proposal contains two unspecified tuning parameters: a positive real valued *h* that controls the length of proposed jumps and a symmetric positive definite matrix $\boldsymbol{M}$ that controls the direction of jumps. Roberts and Rosenthal (2001) showed that the value of *h* that yields optimal asymptotic efficiency has an acceptance rate equal to 0.574. In practice, an algorithm with an acceptance rate between 0.31 and 0.81 is at least 80% efficient (Roberts and Rosenthal 2001,

Theorem 3). MALA typically uses the identity matrix for $\boldsymbol{M}$. Yet in our setting, spline parameters associated to close knots are strongly correlated due to the band structure $\boldsymbol{D}_l^{'}\boldsymbol{D}_l$ in the precision matrix of prior $p(\boldsymbol{\beta}_{lj} \mid \tau_{lj})$. Using the identity matrix limits the mixing of a chain and slows the convergence. Lambert and Eilers (2005) also noted that, by using the identity matrix, the close-knots spline parameters are forced to take similar values, which causes large cross-correlations in a chain. We therefore suggest $\boldsymbol{M} = \boldsymbol{H}_{lj}^{-1}$, where $\boldsymbol{H}_{lj}$ is the Hessian matrix of the negative $\log \pi(\boldsymbol{\beta}_{lj})$ and can be estimated using a "pilot" chain.

Updating spline parameters block-wise is essential to reach convergence for the whole chain. However, separately updating $\boldsymbol{\beta}_{lj}$ and the associated roughness penalty parameter τ_{lj} has yet to provide satisfactory convergence and mixing results (Knorr-Held and Rue 2002; Brezger and Lang 2006). The reason is that the prior for $\boldsymbol{\beta}_{lj}$ depends on τ_{lj} through its precision matrix $\tau_{lj}(\boldsymbol{D}_l^{'}\boldsymbol{D}_l)$. The dependence reflects on the MALA proposal (14) via the gradient of $\pi(\boldsymbol{\beta}_{lj}^{\,t})$; i.e.,

$$\nabla \log \pi(\boldsymbol{\beta}_{lj}^{\,t}) = \nabla \log L(\boldsymbol{\beta}_{lj}^{\,t}) - \tau_{lj}^{t}(\boldsymbol{D}_l^{'}\boldsymbol{D}_l)\boldsymbol{\beta}_{lj}^{\,t}. \quad (16)$$

It should be also noted that the posterior for τ_{lj} is right-skewed with a long tail towards extremely large values. Once the current state τ_{lj}^{t} gets into the tail, causing too large a jump proposed for $\boldsymbol{\beta}_{lj}^{\,t+1}$, the chain quickly becomes stuck in the tail.

To achieve better convergence and mixing properties, this paper uses a joint proposal (Knorr-Held and Rue 2002) for updating spline and roughness penalty parameters in one block. We first sample the candidate τ_{lj}^{*} from a proposal which may depend on the current state τ_{lj}^{t} but not on $\boldsymbol{\beta}_{lj}^{\,t}$. A specific proposal $q(\tau_{lj}^{t}, \tau_{lj}^{*})$ can be constructed by setting $\tau_{lj}^{*} = \tau_{lj}^{t} \cdot z$, where $z \in [1/f, f]$ is random with density $p(z) \propto 1 + 1/z$, and $f > 1$ is a tuning parameter. One advantage of this proposal is that the ratio $q(\tau_{lj}^{*}, \tau_{lj}^{t}) / q(\tau_{lj}^{t}, \tau_{lj}^{*}) = 1$. Conditional on τ_{lj}^{*}, we sample the

candidate $\boldsymbol{\beta}_{lj}^{*}$ from the MALA proposal. This conditional MALA proposal differs from that given by (14) in terms of the gradient term, i.e.,

$$\nabla \log \pi(\boldsymbol{\beta}_{lj}^{t}) = \nabla \log L(\boldsymbol{\beta}_{lj}^{t}) - \tau_{lj}^{*}(\boldsymbol{D}_{l}^{'}\boldsymbol{D}_{l})\boldsymbol{\beta}_{lj}^{t}. \quad (17)$$

The block of candidates $(\boldsymbol{\beta}_{lj}^{*}, \tau_{lj}^{*})$ is accepted with probability

$$\alpha(\boldsymbol{\beta}_{lj}^{t}, \tau_{lj}^{t}, \boldsymbol{\beta}_{lj}^{*}, \tau_{lj}^{*}) = \frac{L(\boldsymbol{\beta}_{lj}^{*})\, p(\boldsymbol{\beta}_{lj}^{*} \mid \tau_{lj}^{*})\, p(\tau_{lj}^{*} \mid \delta_{lj}^{t})}{L(\boldsymbol{\beta}_{lj}^{t})\, p(\boldsymbol{\beta}_{lj}^{t} \mid \tau_{lj}^{t})\, p(\tau_{lj}^{t} \mid \delta_{lj}^{t})} \cdot \frac{q(\boldsymbol{\beta}_{lj}^{*}, \boldsymbol{\beta}_{lj}^{t})}{q(\boldsymbol{\beta}_{lj}^{t}, \boldsymbol{\beta}_{lj}^{*})}, \quad (18)$$

with $p(\tau_{lj} \mid \delta_{lj})$ give in (9), $q(\boldsymbol{\beta}_{lj}^{t}, \boldsymbol{\beta}_{lj}^{*})$ conditional on τ_{lj}^{*}, and $q(\boldsymbol{\beta}_{lj}^{*}, \boldsymbol{\beta}_{lj}^{t})$ on τ_{lj}^{t}.

4 Simulation Study

We conducted a simulation study with a focus on evaluating the model performance for time-varying coefficients with different curvatures in both low and high event rate data settings. Simulated data were generated from a Poisson process with conditional intensity:

$$\lambda_{ij}(t \mid \boldsymbol{x}_i, \boldsymbol{z}_i, b_{ij}) = \exp\{x_{i1}\alpha_{1j} + \beta_{0j}(t) + z_{i1}\beta_{1j}(t) + z_{i2}\beta_{2j}(t) + b_{ij}\}, 0 \le t \le 10.$$

We considered I = 500 processes and J = 2 event types. The censoring time was generated from a gamma distribution independent of the process. Each process was censored at the maximum follow-up time of 10, if not censored before. The covariate x_{i1} was generated from a uniform distribution on $[-1,1]$. The coefficient was set to $\alpha_{11} = 0.5$ for event type j = 1 and $\alpha_{12} = -0.5$ for event type j = 2. The covariates z_{i1} and z_{i2} were binary with probability density $p(z_{i1}, z_{i2}) = (1-p_1-p_2)^{1-z_{i1}-z_{i2}}\, p_1^{z_{i1}}\, p_2^{z_{i2}}$, where $0 \le z_{i1} + z_{i2} \le 1$ and $p_1 = p_2 = 1/3$. The time-varying coefficients for event type j = 1 were functions of low curvature (shown in Figure 1(a)): a quadratic function $\beta_{11}(t) = -0.1(t-4.75)^2 + 1.5$, and a sinusoidal function $\beta_{21}(t) = \sin(0.2\pi t)$. The time-varying coefficients for event type j = 2 were functions of high curvature (shown in Figure 1(b)):

$$\beta_{12}(t) = \frac{8}{1+e^{-1.05(t-3.5)}} + \frac{8}{1+e^{(t-4.5)}} + \frac{8}{1+e^{(t-5.5)}} + \frac{8}{1+e^{-1.05(t-6.5)}} - 16,$$
$$\beta_{22}(t) = \cos(1/3\pi(t+1)) + 0.01t^2.$$

There are two settings for the log baseline intensities $\beta_{0j}(t)$:

(1) a low event rate setting: $\beta_{01}(t) = 0.1t - 3.35$ and $\beta_{02}(t) = 0.01(t-4)^2 - 2.75$;
(2) a high event rate setting: $\beta_{0j}(t)$ increased by one unit from the low event rate setting, j = 1, 2.

The random effect $\boldsymbol{b_i} = (b_{i1}, b_{i2})'$ was generated from a multivariate normal distribution with mean $\mathbf{0}$ and covariance matrix $\boldsymbol{\Sigma}$. The diagonal entries of $\boldsymbol{\Sigma}$ were $\sigma_{11} = \sigma_{22} = 1$. There were three settings for the off-diagonal entry, $\sigma_{12} = 0.2$, 0.5, and 0.8, corresponding to a low, moderate and high correlation between event types.

We simulated 500 replications under each parameter setting. In the low event rate setting, the average number of events per process was one for each type; in the high event rate setting, the average number of events per process was three for each type. The unknown functions were approximated by 10 cubic B-splines; the order in the prior for spline parameters was r = 2. We fitted each replicate data set in two ways: (1) using splines for $\beta_{lj}(t)$ only; (2) using splines for $\beta_{lj}(t)$ and α_{1j}. For each data set, a final chain of length $8,000$ was generated after tuning of parameters to ensure an satisfactory acceptance rate.

Figures 1 and 2 display the simulation results of using splines to approximate $\beta_{lj}(t)$ and α_{1j} under parameter setting $\sigma_{12} = 0.2$. Figure 1 corresponds to low event rate data with one event per process on average, and Figure 2 corresponds to high event rate data with three events per process on average. For low-curvature time-varying coefficients, the bias of spline fit is typically negligible for low event rate data, except that the posterior mean (shown in Figure 1(a)) for sinusoidal function $\beta_{21}(t)$ does deviate slightly at the end of the

follow-up time. Similar bias for $\beta_{21}(t)$ also occurs for low event rate data with $\sigma_{12} = 0.5$ and 0.8. However, as shown in Figure 2(a), such bias is no longer noticeable for high event rate data. The simulation results for high-curvature time-varying coefficients are similar: small bias occurs around the bumps of $\beta_{12}(t)$ and $\beta_{22}(t)$ for low event rate data, and is greatly diminished for high event rate data. The spline fits for the log baseline intensities are overall close to the true value, though there is some bias in $\beta_{02}(t)$ at the boundaries. For constant coefficients α_{1j}, event rate does not affect the spline fit—no noticeable bias for α_{1j} exists under either event rate setting.

Tables 1 and 2 show the simulation results for Σ and α_{1j}. The relative bias (RB; %) was obtained from the bias divided by the true parameter value. Its absolute value is below 2% for low event rate data (except for $\sigma_{12} = 0.2$) and even smaller for high event rate data. The mean of standard error (SEM; the mean of posterior standard deviations) is extremely close to the empirical standard error (SE; the standard error of posterior means). The coverage probability (CP; %) for 95% credible interval is roughly at the nominal level.

In summary, the proposed model performs well under various settings. The bias is small for time-varying coefficients of low and high curvature as well as for parametric coefficients. The credible intervals have appropriate coverage probabilities.

5 Application: Evaluating the Impact of Sleep on Driving Performance and Safety for Truck Drivers

Sleep time prior a driving shift is a critical factor affecting driver fatigue (Hanowski et al. 2007). Literature also shows that whether or not a driver is well rested prior to a long on-duty shift directly impacts driver fatigue and driving performance (Banks et al. 2007; Lim and Dinges 2008, 2010). We used the approach developed in this paper to assess the temporal profile of driving performance over a driving shift and the effect of off-duty sleep time on this temporal profile.

We applied the proposed method to data collected by the Commercial Truck Driver Naturalistic Driving Study (Blanco et al. 2011). The study recruited 100 drivers from four for-hire trucking companies. Each driver drove an instrumented truck for about one month. Driving data were recorded at high frequency by an unobtrusive data-collection equipment installed on the trucks. In addition, each driver was required to report the beginning and ending times for on- and off-duty activities in a daily activity register form. The form included activities such as sleep, break, working, driving, etc.

Studies have shown that total off-duty sleep time is considered insufficient if the total off-duty sleep duration is less than 7 hours (Van Dongen, Rogers and Dinges 2003; Van Dongen, Maislin, Mullington and Dinges 2003). In the following analyses, we considered sleep time as normal if the off-duty sleep duration was between 7 and 9 hours, and sleep time as abundant if it was more than 9 hours.

Events of interest were safety-critical events identified in the study. Since only a very small number of crashes and near-crashes were observed, we combined crashes, near-crashes, and crash-relevant conflicts (CRC) in to one event type. Previous study has shown similarities among certain types of safety-critical event (Guo et al. 2010). The second event type was unintentional lane deviation (ULD), which has been shown to be a measure of driving performance decrement and that it is sensitive to driving fatigue (Hanowski et al. 2008; van Dongen et al. 2010). Driving performance was assessed in two time scales: driving time since a shift started (see Section 5.1) and driving time from one break until the next break in a shift (see Section 5.2).

5.1 Within-shifts driving performance

To evaluate the impact of sleep time on the driving performance in the succeeding long shift, we organized the data into pairs of an off-duty period followed by an on-duty period. The off-duty period was set to be sufficiently long

(at least 10 hours or including sleep time for more than 7 hours) such that the beginning of a following on-duty period was a “fresh start” for the driver. Since some off-duty periods spanned several days or even weeks, sleep duration in a 12-hour time window right before an on-duty period was used in analysis. For each on-duty period, episodes of driving tasks were connected in time to construct a continuous driving period in a shift. Due to the 11-hour driving limit set by the Federal Motor Carrier Safety Administration, driving time in a shift longer than 11 hours was truncated. We refer to Liu et al. (2019) for more details on data preparation.

The analysis dataset includes $1{,}880$ shifts: 20.6% (388) of the shifts with insufficient sleep (< 7 hours) prior to the driving shift, 58.2% ($1{,}095$) with normal sleep (7–9 hours), and 21.1% (397) with abundant sleep (≥ 9 hours). Figure 3 displays the event rate in the 1st–11th driving hours from the beginning of a shift by sleep time group. For the ith driving hour, where $i = 1, \ldots, 11$, the number of events was counted; the exposure (time in hours) was the sum of all shifts' driving duration that occurred in the ith driving hour; the event rate corresponding to the ith driving hour was calculate as the ratio of the event count to the exposure. As shown in Figure 3, for crashes, near-crashes and CRC, the difference between insufficient, normal and abundant sleep time is not noticeable until the 10th–11th driving hours. For ULD, the event rate of insufficient sleep is above that of normal sleep in the 8th–11th driving hours, and the rate of abundant sleep also climbs in the last 2 driving hours.

We applied the proposed method to the data, where each continuous driving period in a shift was treated as an event process. Two dummy variables were created for indicating insufficient and abundant sleep time, and were assumed to have time-varying coefficients. The baseline intensities (normal sleep) and time-varying coefficients were estimated by 10 cubic B-splines; the order in the prior for spline parameters was $r = 2$. After tuning of parameters to ensure a satisfactory acceptance rate, a final chain of length $20{,}000$ was generated. Table

3 shows the results for the dependence structure between the two event types. It shows significant evidence that crashes, near-crashes and CRC are positively correlated with ULD.

Figure 4 shows the log baseline intensities and time-varying coefficients evaluated at the posterior mean along with 95% pointwise credible intervals. The time-varying coefficient of insufficient/abundant sleep provides a temporal profile of the difference between the insufficient/abundant and normal sleep groups. For crashes, near-crashes, and CRC, Figure 4 does not show significant difference between the three sleep time groups. However, for ULD events, Figure 4 shows that the coefficient functions of both insufficient and abundant sleep start to rise above zero after the 8th driving hour and keep increasing until the end of the shift. The results indicate that, compared to normal sleep time, drivers with insufficient and abundant sleep prior to a shift have a significantly higher ULD risk after 8 hours of driving.

It is interesting to observe that for ULD events, there is a declining trend in the log baseline (normal sleep) intensity in the later part of a driving shift (Figure 4). While this seems does not fit patterns of monotonic increase in intensity, it should be noted that many other factors also affect driving performance in a long shift—one important factor being drivers' break behavior. As shown in Liu et al. (2019), drivers with normal sleep time tended to have longer breaks after the 8th driving hour, which could cause the baseline intensity to decline in the same time range. Compared to normal sleep time, drivers with abundant sleep had much shorter breaks over the whole driving time, which could be the reason for the corresponding coefficient function to climb in the later part of a driving shift. After the 8th driving hour, drivers with insufficient sleep had the longest break length among the three sleep time groups. However, within the same time range, their coefficient function is above zero and keeps increasing as driving goes on. This implies that longer breaks in the later part of a driving shift are not sufficient to compensate for lack of sleep prior to the shift.

5.2 Between-breaks driving performance

The previous analysis assesses the temporal profile of driving performance in a long shift, which is shown to have a complex relationship between sleep time and drivers' break activities. In this section, we evaluate driving performance from one shift break until the next shift break. We considered a break as a short-time activity (no more than 5 hours) which does not involve driving or on-duty work. Between-breaks driving time longer than 3 hours was truncated due to insufficient exposure. Of the $1,286$ between-breaks driving sections extracted from the $1,880$ shifts described in Section 5.1, 14.3% (184) were associated with insufficient sleep, 60.5% (778) were associated with normal sleep, and 25.2% (324) were associated with abundant sleep.

Figure 5 displays the between-breaks event rate in every half an hour for these three sleep time groups. For crashes, near-crashes, and CRC, the event rate of insufficient sleep starts to rise above the other two groups from the second driving hour after a break; the rate of abundant sleep stays above the normal group in the first 2 driving hours. For ULD, the insufficient sleep group has a substantially higher event rate than the other two groups over the whole between-breaks driving section, while the event rates of both the normal and abundant sleep groups remains low at around 0.1.

We applied the proposed method to the between-breaks data, where each between-breaks driving section was treated as an event process. The fitted dependence structure between the two event types are in Table 3. The event types are also positively correlated.

Figure 6 shows the log baseline (normal sleep) intensities and time-varying coefficients evaluated at the posterior mean with 95% pointwise credible intervals. Due to the short length of between-breaks driving sections, the intensities for the normal sleep group do not contain significant time-varying patterns. However, for crashes, near-crashes and CRC, the coefficient function

of insufficient sleep starts to rise above zero after 1.5 driving hours and keeps increasing as driving goes on; the coefficient function of abundant sleep is significantly greater than zero in the first 2 driving hours. These results are consistent with Figure 5. This indicates that, after taking a break, drivers with insufficient sleep time have a higher risk of crashes, near-crashes and CRC after 1.5 driving hours as compared to those with normal sleep time. Drivers with abundant sleep also have a significantly higher risk in the first 2 driving hours after a break, though there is no sufficient evidence showing the trend of their risk after the second driving hour. For ULD events, there is no significant result for the coefficient of abundant sleep. However, the coefficient function of insufficient sleep remains significantly above zero over the entire between-breaks driving section. This suggests that, compared to normal sleep time, drivers with insufficient sleep prior to a shift have a higher ULD risk even after taking a break. This result is consistent with that found in Section 5.1 for the difference in ULD risk between insufficient and normal sleep groups.

6 Summary and Discussion

Assessing the temporal profiles for recurrence rate and covariate effects is of common interest in studies with multi-type recurrent events. This paper proposes a Bayesian joint model based on multivariate log-normal frailties for recurrent event data and incorporates time-varying coefficients for analyzing the temporal covariate effects. The Bayesian penalized splines approach is used to achieve smooth estimation for both time-varying coefficients and the baseline intensity. Adopting a robust prior specification approach provides the desired flexibility for the spline fit and achieves an objective fitting procedure without the need for the subjective choice of hyperparameters. Furthermore, MALA algorithms integrated in a joint sampling scheme help achieve better convergence and mixing properties and address the issue of strong dependence between spline and roughness penalty parameters in the posterior sampling. The simulation study demonstrates a good model performance for estimating low- and high-curvature

time-varying coefficients; the model performs consistently well for data with low and high event rates.

There are several possible extensions of the current research. The paper chooses multivariate normal distribution for frailty since it provides flexibility on the dependence structure among different event types. Another approach to relax the frailty assumption is through the nonparametric frailty distribution (Fan 1991; Chen 1995; Carroll and Hall 1988). In Section 5, only one frailty term is used to account for heterogeneity at the shift level. However, there might be heterogeneity existing at the driver level. A nested frailty model with random effects for both levels is worth pursuing yet requires a larger sample size. To model different event types, an alternative is to use competing risk models (Fine and Gray 1999; Gichangi and Vach 2005). Section 5.1 has mentioned that driver' s break behavior is an important factor affecting driving performance. Other factors of driving performance include caffeine intake, breaks and rest, as well as time of day. How to incorporate or adjust these factors is worth investigating.

The application to the Commercial Truck Driver Naturalistic Driving Study shows that unintentional lane deviation is positively correlated with crashes, near-crashes and crash relevant conflicts. The results from analyzing within-shifts data reveal that lack of sleep has a negative impact on driving performance, measured by unintentional lane deviation, after 8 hours of driving in a shift. The results also imply a complex relationship between sleep time, the driver's choice to take breaks while on duty, and driving performance. The analysis for between-breaks data shows consistent evidence that, after taking a break, insufficient sleep still corresponds to a significantly higher intensity for unintentional lane deviation and crashes, near-crashes and crash relevant conflicts. These findings provide useful information for truck driver fatigue management and hours-of-service regulation. In addition to the findings for commercial truck drivers, the results provide an illustration and sugguest a wide applicability of the proposed method to epidemiological and clinic studies.

References

Aalen, O. (1978), 'Nonparametric inference for a family of counting processes', *The Annals of Statistics* **6**(4), 701–726.

Abu-Libdeh, H., Turnbull, B. W. and Clark, L. C. (1990), 'Analysis of multi-type recurrent events in longitudinal studies; application to a skin cancer prevention trial', *Biometrics* **46**(4), 1017–1034.

Amorim, L. D., Cai, J., Zeng, D. and Barreto, M. L. (2008), 'Regression splines in the time-dependent coefficient rates model for recurrent event data', *Statistics in Medicine* **27**(28), 5890–5906.

Banks, S., Dinges, D. F. et al. (2007), 'Behavioral and physiological consequences of sleep restriction', *J Clin Sleep Med* **3**(5), 519–528.

Blanco, M., Hanowski, R. J., Olson, R. L., Morgan, J. F., Soccolich, S. A., Wu, S.-C. and Guo, F. (2011), The impact of driving, non-driving work, and rest breaks on driving performance in commercial motor vehicle operations, Technical Report FMCSA-RRR-11-017, Federal Motor Carrier Safety Administration, Washington, DC.

Brezger, A. and Lang, S. (2006), 'Generalized structured additive regression based on bayesian P-splines', *Computational Statistics & Data Analysis* **50**(4), 967–991.

Cai, J. and Schaubel, D. E. (2004), 'Marginal means/rates models for multiple type recurrent event data', *Lifetime Data Analysis* **10**(2), 121–138.

Cai, T. and Betensky, R. A. (2003), 'Hazard regression for interval-censored data with penalized spline', *Biometrics* **59**(3), 570–579.

Cai, T., Hyndman, R. J. and Wand, M. P. (2002), 'Mixed model-based hazard estimation', *Journal of Computational and Graphical Statistics* **11**(4), 784–798.

Cai, Z., Fan, J. and Li, R. (2000), 'Efficient estimation and inferences for varying-coefficient models', *Journal of the American Statistical Association* **95**(451), 888–902.

Carroll, R. J. and Hall, P. (1988), 'Optimal rates of convergence for deconvolving a density', *Journal of the American Statistical Association* **83**(404), 1184–1186.

Carroll, R. J., Ruppert, D. and Welsh, A. H. (1998), 'Local estimating equations', *Journal of the American Statistical Association* **93**(441), 214–227.

Chen, B. E. and Cook, R. J. (2009), 'The analysis of multivariate recurrent events with partially missing event types', *Lifetime Data Analysis* **15**(1), 41–58.

Chen, B. E., Cook, R. J., Lawless, J. F. and Zhan, M. (2005), 'Statistical methods for multivariate interval-censored recurrent events', *Statistics in Medicine* **24**(5), 671–691.

Chen, C. and Guo, F. (2016), 'Evaluating the influence of crashes on driving risk using recurrent event models and naturalistic driving study data', *Journal of Applied Statistics* **43**(12), 2225–2238.

Chen, J. (1995), 'Optimal rate of convergence for finite mixture models', *The Annals of Statistics* **23**(1), 221–233.

Chen, Z. and Dunson, D. B. (2003), 'Random effects selection in linear mixed models', *Biometrics* **59**(4), 762–769.

Cook, R. J. and Lawless, J. F. (2007), *The Statistical Analysis of Recurrent Events*, Springer, New York, NY.

Dingus, T. A., Guo, F., Lee, S., Antin, J. F., Perez, M., Buchanan-King, M. and Hankey, J. (2016), 'Driver crash risk factors and prevalence evaluation using

naturalistic driving data', *Proceedings of the National Academy of Sciences of the United States of America* **113**(10), 2636–2641.

Dingus, T. A., Hankey, J. M., Antin, J. F., Lee, S. E., Eichelberger, L., Stulce, K. E., McGraw, D., Perez, M. and Stowe, L. (2015), Naturalistic driving study: Technical coordination and quality control, Report SHRP 2 Report S2-S06-RW-1, Transportation Research Board, National Academies.

Eilers, P. H. C. and Marx, B. D. (1996), 'Flexible smoothing with B-splines and penalties', *Statistical Science* **11**(2), 89–102.

Fahrmeir, L. and Lang, S. (2001), 'Bayesian inference for generalized additive mixed models based on Markov random field priors', *Journal of the Royal Statistical Society: Series C (Applied Statistics)* **50**(2), 201–220.

Fan, J. (1991), 'On the optimal rates of convergence for nonparametric deconvolution problems', *The Annals of Statistics* **19**(3), 1257–1272.

Fan, J. and Zhang, W. (1999), 'Statistical estimation in varying coefficient models ', *The Annals of Statistics* **27**(5), 1491–1518.

Fine, J. P. and Gray, R. J. (1999), 'A proportional hazards model for the subdistribution of a competing risk', *Journal of the American statistical association* **94**(446), 496–509.

Friedman, M. (1982), 'Piecewise exponential models for survival data with covariates', *The Annals of Statistics* **10**(1), 101–113.

Gichangi, A. and Vach, W. (2005), 'The analysis of competing risks data: A guided tour', *Statistics in Medicine* **132**, 1–14.

Golub, G. H. and Van Loan, C. F. (1983), *Matrix Computations*, The Johns Hopkins University Press, Baltimore, MD.

Guo, F. (2019), 'Statistical methods for naturalistic driving studies', *Annual Review of Statistics and Its Application* **6**(1), 309–328.

Guo, F. and Fang, Y. (2013), 'Individual driver risk assessment using naturalistic driving data', *Accident Analysis & Prevention* **61**, 3–9.

Guo, F., Klauer, S. G., Fang, Y., Hankey, J. M., Antin, J. F., Perez, M. A., Lee, S. E. and Dingus, T. A. (2017), 'The effects of age on crash risk associated with driver distraction', *International Journal of Epidemiology* **46**(1), 258–265.

Guo, F., Klauer, S., Hankey, J. and Dingus, T. (2010), 'Near crashes as crash surrogate for naturalistic driving studies', *Transportation Research Record: Journal of the Transportation Research Board* **2147**, 66–74.

Guo, F., Simons-Morton, B. G., Klauer, S. E., Ouimet, M. C., Dingus, T. A. and Lee, S. E. (2013), 'Variability in crash and near-crash risk among novice teenage drivers: A naturalistic study', *The Journal of pediatrics* **163**(6), 1670–1676.

Hanowski, R. J., Bowman, D., Alden, A., Wierwille, W. W. and Carroll, R. (2008), PERCLOS+: Moving beyond single-metric drowsiness monitors, Technical Report 2008-01-2692, SAE Technical Paper.

Hanowski, R. J., Hickman, J., Fumero, M. C., Olson, R. L. and Dingus, T. A. (2007), 'The sleep of commercial vehicle drivers under the 2003 hours-of-service regulations', *Accident Analysis & Prevention* **39**(6), 1140–1145.

Hastie, T. and Loader, C. (1993), 'Local regression: Automatic kernel carpentry', *Statistical Science* **8**(2), 120–129.

Hastie, T. and Tibshirani, R. (1993), 'Varying-coefficient models', *Journal of the Royal Statistical Society. Series B (Methodological)* **55**(4), 757–796.

Huang, J. Z., Wu, C. O. and Zhou, L. (2002), 'Varying-coefficient models and basis function approximations for the analysis of repeated measurements', *Biometrika* **89**(1), 111–128.

Jayaram, L., Pizzichini, M. M., Cook, R. J., Boulet, L.-P., Lemière, C., Pizzichini, E., Cartier, A., Hussack, P., Goldsmith, C. H., Laviolette, M., Parameswaran, K. and Hargreave, F. E. (2006), 'Determining asthma treatment by monitoring sputum cell counts: effect on exacerbations', *European Respiratory Journal* **27**(3), 483–494.

Jullion, A. and Lambert, P. (2007), 'Robust specification of the roughness penalty prior distribution in spatially adaptive Bayesian P-splines models', *Computational Statistics & Data Analysis* **51**(5), 2542–2558.

Kauermann, G. (2005), 'Penalized spline smoothing in multivariable survival models with varying coefficients', *Computational Statistics & Data Analysis* **49**(1), 169–186.

Klauer, S. G., Guo, F., Simons-Morton, B. G., Ouimet, M. C., Lee, S. E. and Dingus, T. A. (2014), 'Distracted driving and risk of road crashes among novice and experienced drivers', *New England Journal of Medicine* **370**(1), 54–59.

Knorr-Held, L. and Rue, H. (2002), 'On block updating in markov random field models for disease mapping', *Scandinavian Journal of Statistics* **29**(4), 597–614.

Lambert, P. and Eilers, P. H. C. (2005), 'Bayesian proportional hazards model with time-varying regression coefficients: a penalized Poisson regression approach', *Statistics in Medicine* **24**(24), 3977–3989.

Lang, S. and Brezger, A. (2004), 'Bayesian P-splines', *Journal of Computational and Graphical Statistics* **13**(1), 183–212.

Li, Q., Guo, F., Kim, I., Klauer, S. G. and Simons-Morton, B. G. (2018), 'A bayesian finite mixture change-point model for assessing the risk of novice teenage drivers', *Journal of Applied Statistics* **45**(4), 604–625.

Li, Q., Guo, F., Klauer, S. G. and Simons-Morton, B. G. (2017), 'Evaluation of risk change-point for novice teenage drivers', *Accident Analysis & Prevention* **108**, 139–146.

Lim, J. and Dinges, D. F. (2008), 'Sleep deprivation and vigilant attention', *Annals of the New York Academy of Sciences* **1129**(1), 305–322.

Lim, J. and Dinges, D. F. (2010), 'A meta-analysis of the impact of short-term sleep deprivation on cognitive variables.', *Psychological Bulletin* **136**(3), 375–389.

Lin, L.-A., Luo, S., Chen, B. E. and Davis, B. R. (2017), 'Bayesian analysis of multi-type recurrent events and dependent termination with nonparametric covariate functions', *Statistical Methods in Medical Research* **26**(6), 2869–2884.

Liu, Y., Guo, F. and Hanowski, R. J. (2019), 'Impact of sleep time on truck driver performance over long driving shift', *Statistics in Medicine*. In Press.

Ng, E. T. M. and Cook, R. J. (1999), 'Robust inference for bivariate point processes', *Canadian Journal of Statistics* **27**(3), 509–524.

Nielsen, J. D. and Dean, C. B. (2005), 'Regression splines in the quasi-likelihood analysis of recurrent event data', *Journal of Statistical Planning and Inference* **134**(2), 521–535.

Pourahmadi, M. (1999), 'Joint mean-covariance models with applications to longitudinal data: Unconstrained parameterisation', *Biometrika* **86**(3), 677–690.

Roberts, G. O. and Rosenthal, J. S. (2001), 'Optimal scaling for various Metropolis-Hastings algorithms', *Statistical Science* **16**(4), 351–367.

Roberts, G. O. and Tweedie, R. L. (1996), 'Exponential convergence of Langevin distributions and their discrete approximations', *Bernoulli* **2**(4), 341–363.

Rue, H. (2001), 'Fast sampling of Gaussian Markov random fields', *Journal of the Royal Statistical Society: Series B (Statistical Methodology)* **63**(2), 325–338.

Sun, L., Zhou, X. and Guo, S. (2011), 'Marginal regression models with time-varying coefficients for recurrent event data', *Statistics in Medicine* **30**(18), 2265–2277.

van Dongen, H. P. A., Jackson, M. L. and Belenky, G. (2010), *Duration Restart Period Needed to Recycle with Optimal Performance: Phase II*, US Department of Transportation, Federal Motor Carrier Safety Administration, Office of Analysis, Research and Technology.

Van Dongen, H. P., Maislin, G., Mullington, J. M. and Dinges, D. F. (2003), 'The cumulative cost of additional wakefulness: dose-response effects on neurobehavioral functions and sleep physiology from chronic sleep restriction and total sleep deprivation', *Sleep* **26**(2), 117–126.

Van Dongen, H., Rogers, N. L. and Dinges, D. F. (2003), 'Sleep debt: Theoretical and empirical issues', *Sleep and Biological Rhythms* **1**(1), 5–13.

Yu, Z., Liu, L., Bravata, D. M., Williams, L. S. and Tepper, R. S. (2013), 'A semiparametric recurrent events model with time-varying coefficients', *Statistics in Medicine* **32**(6), 1016–1026.

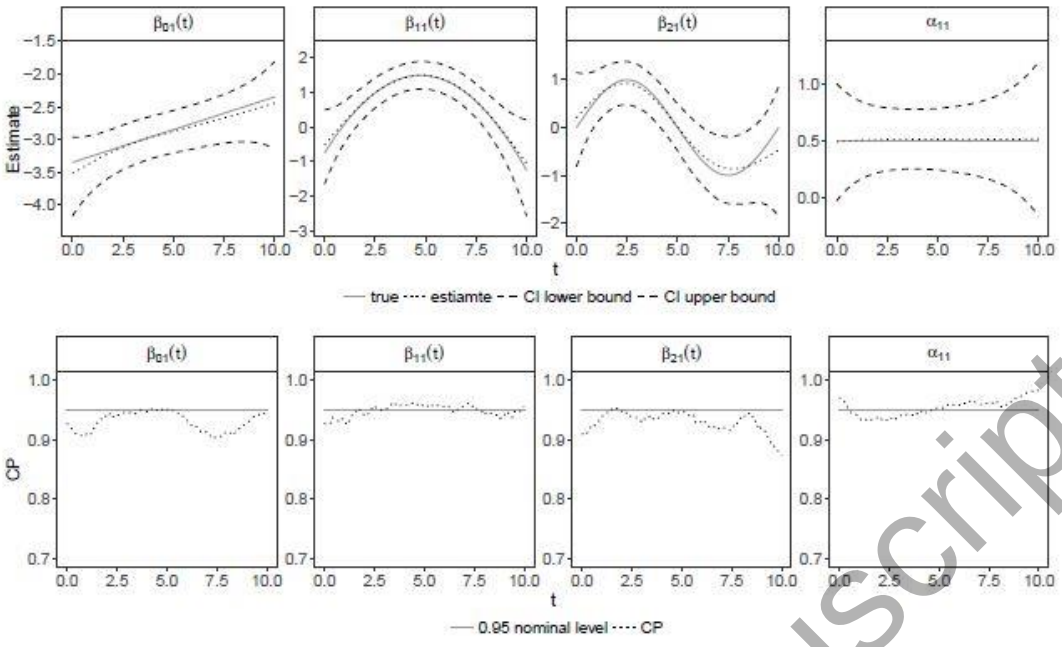

(a) Event type $j = 1$: time-varying coefficients of low curvature.

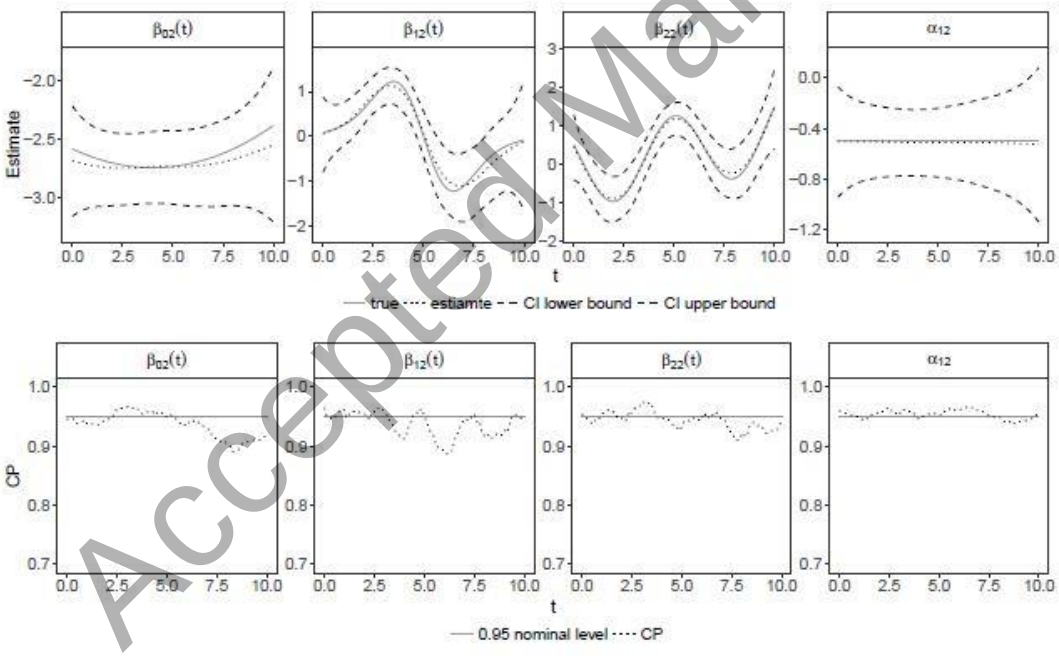

(b) Event type $j = 2$: time-varying coefficients of high curvature.

Fig. 1 Estimates, 95% credible intervals (CIs) and coverage probability (CP) for coefficients $\beta_{lj}(t)$ and α_{1j} under the simulation setting of $\sigma_{12} = 0.2$ and low event rate.

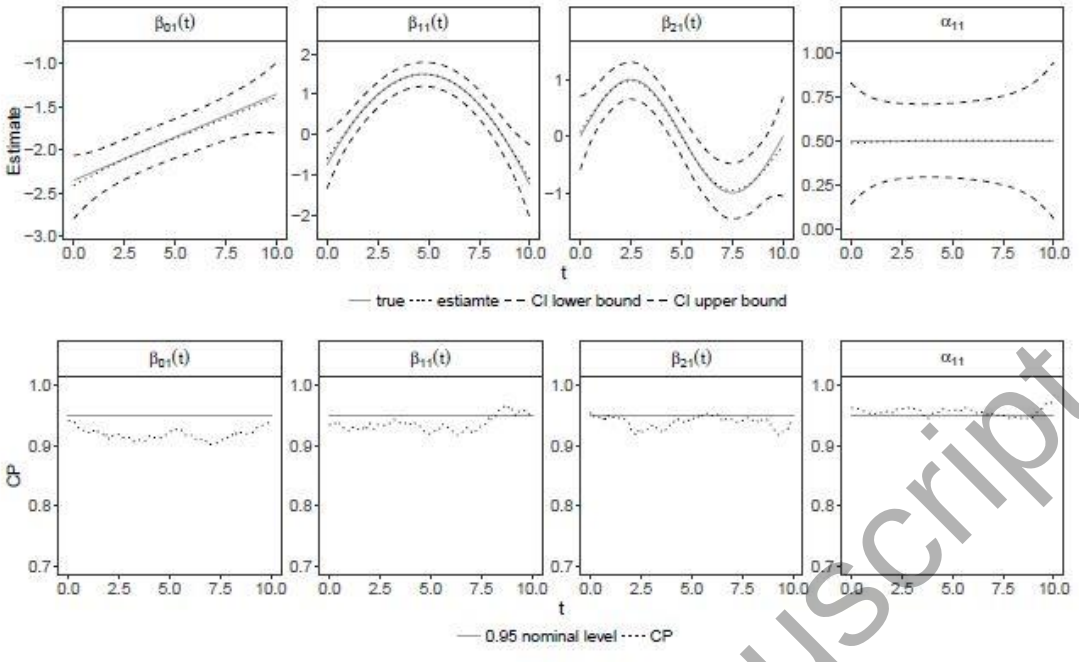

(a) Event type $j = 1$: time-varying coefficients of low curvature.

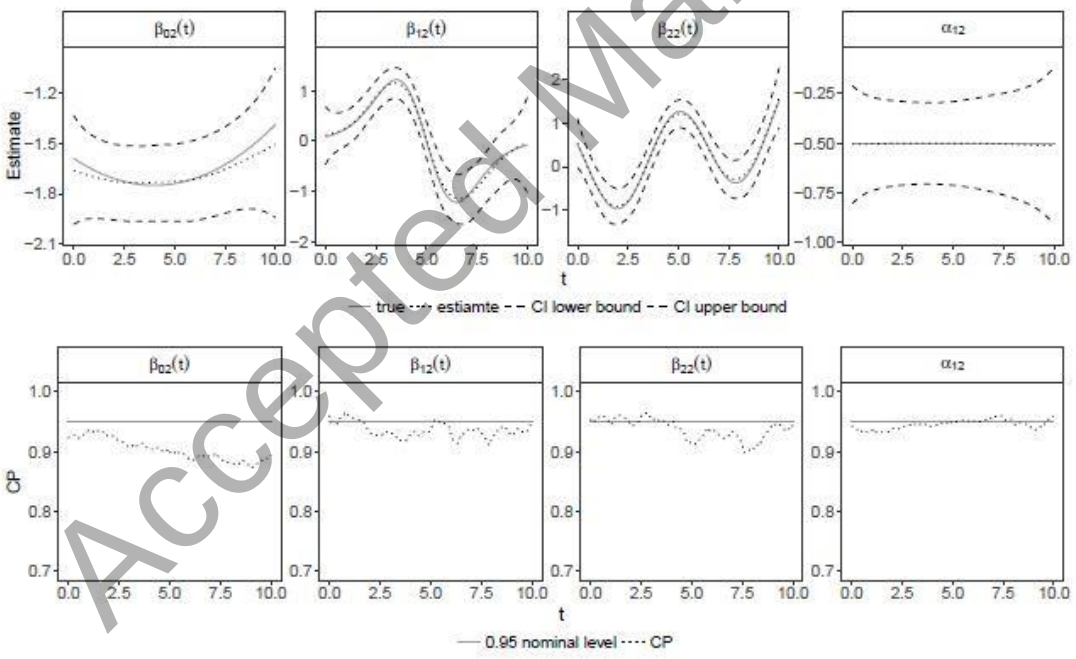

(b) Event type $j = 2$: time-varying coefficients of high curvature.

Fig. 2 Estimates, 95% credible intervals (CIs) and coverage probability (CP) for coefficients $\beta_{lj}(t)$ and α_{1j} under the simulation setting of $\sigma_{12} = 0.2$ and high event rate.

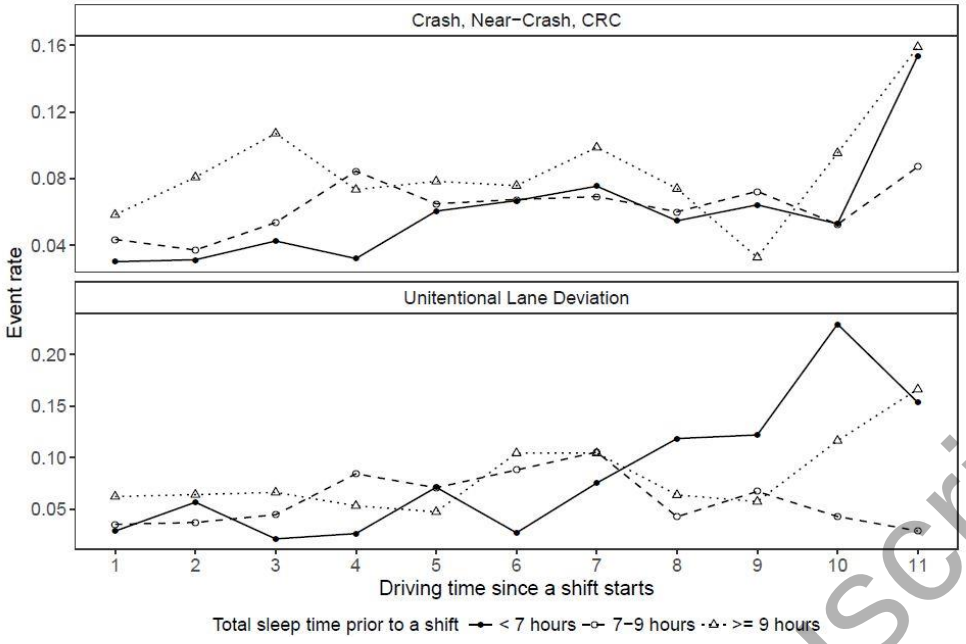

Fig. 3 Within-shifts driving performance: the event rate in the 1st–11th driving hours by sleep time group.

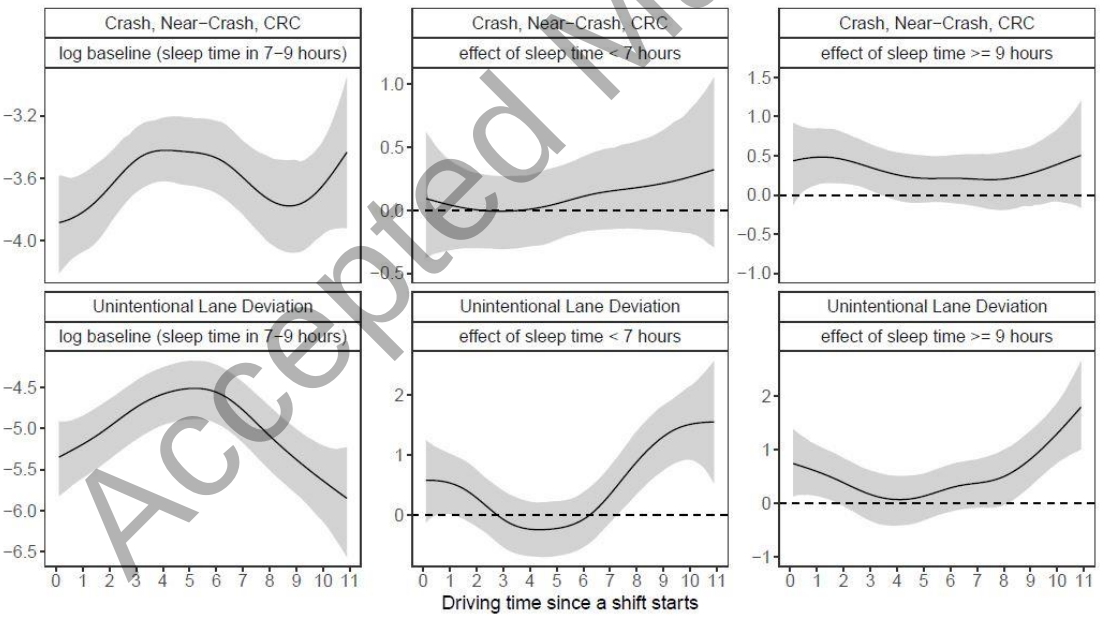

Fig. 4 Within-shifts driving performance. The log baseline (sleep time in 7–9 hours) intensities and time-varying effects of insufficient (sleep time < 7 hours) and abundant sleep (sleep time ≥ 9 hours): posterior mean (solid line), 95% pointwise credible interval (shaded gray area).

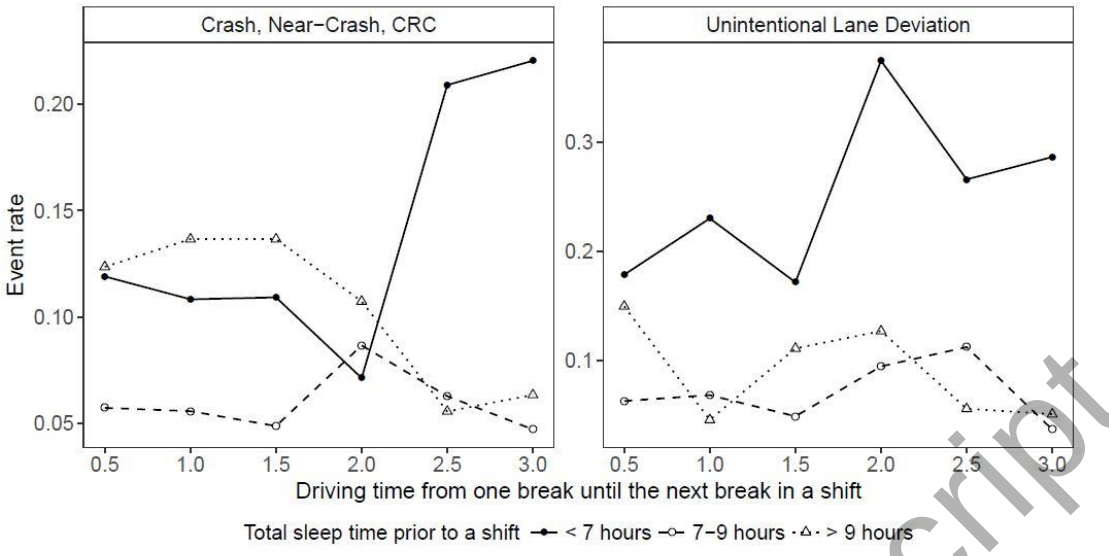

Fig. 5 Between-breaks driving performance: the event rate in every half an hour by sleep time group.

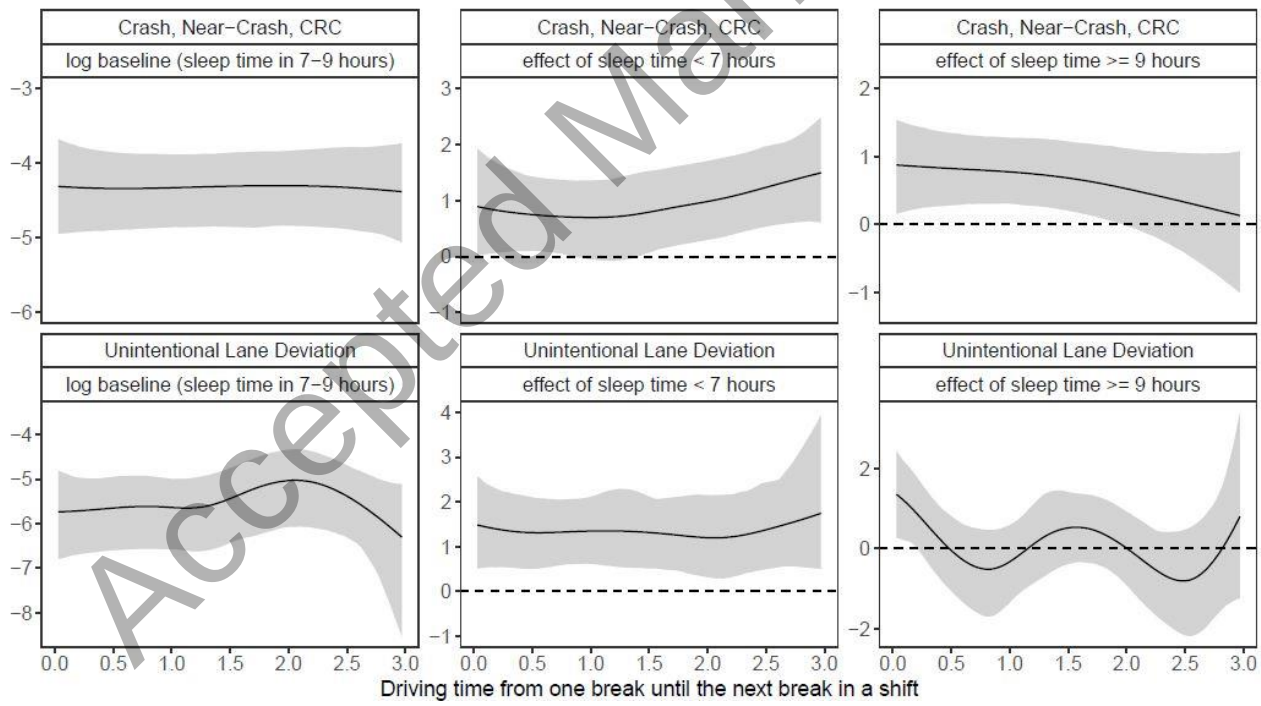

Fig. 6 Between-breaks driving performance. The log baseline (sleep time in 7–9 hours) intensities and time-varying effects of insufficient (sleep time < 7 hours) and abundant sleep (sleep time ≥ 9 hours): posterior mean (solid line), 95% pointwise credible interval (shaded gray area).

Table 1 Simulation results for α_{1j} and Σ. Splines were used to approximate $\beta_{lj}(t)$.

		Low Event Rate					High Event Rate				
	True	Mean	RB[a]	SE[b]	SEM[c]	CP[d]	Mean	RB	SE	SEM	CP
α_{11}	0.5	0.504	0.8	0.124	0.124	94.4	0.500	0.1	0.095	0.101	97.2
α_{12}	–0.5	–0.507	1.4	0.125	0.122	94.4	–0.502	0.4	0.103	0.101	94.6
σ_{11}	1.0	1.010	1.0	0.077	0.076	96.0	1.007	0.7	0.053	0.055	94.8
σ_{12}	0.2	0.189	–5.4	0.101	0.103	95.0	0.201	0.3	0.069	0.070	95.6
σ_{22}	1.0	1.016	1.6	0.076	0.076	93.6	1.012	1.2	0.051	0.054	96.8
α_{11}	0.5	0.492	–1.7	0.115	0.124	96.0	0.505	0.9	0.101	0.103	95.0
α_{12}	–0.5	–0.505	1.0	0.123	0.123	94.8	–0.509	1.8	0.107	0.101	92.6
σ_{11}	1.0	1.007	0.7	0.077	0.075	93.0	1.012	1.2	0.056	0.055	92.8
σ_{12}	0.5	0.494	–1.2	0.091	0.090	96.0	0.500	0.0	0.060	0.059	93.6
σ_{22}	1.0	1.019	1.9	0.076	0.076	94.0	1.006	0.6	0.053	0.054	95.2
α_{11}	0.5	0.510	1.9	0.124	0.124	94.2	0.503	0.5	0.101	0.101	93.8
α_{12}	–0.5	–0.510	1.9	0.119	0.122	95.0	–0.501	0.2	0.102	0.101	93.8
σ_{11}	1.0	1.011	1.1	0.076	0.074	93.4	1.000	–0.0	0.084	0.053	94.0
σ_{12}	0.8	0.796	–0.4	0.071	0.068	93.8	0.789	–1.4	0.116	0.039	92.2
σ_{22}	1.0	1.007	0.7	0.074	0.073	95.2	1.007	0.7	0.053	0.053	94.4

[a] Relative bias (%), obtained from the bias divided by the true value.

[b] Empirical standard error; i.e., the standard error of posterior means.

[c] Mean standard error; i.e., the mean of posterior standard deviations.

[d] Coverage probability (%) for 95% credible intervals.

Table 2 Simulation results for Σ. Splines were used to approximate $\beta_{lj}(t)$ and α_{1j}.

		Low Event Rate					High Event Rate				
	True	Mean	RB[a]	SE[b]	SEM[c]	CP[d]	Mean	RB	SE	SEM	CP
σ_{11}	1.0	1.010	1.0	0.077	0.076	94.2	1.008	0.7	0.054	0.055	94.2
σ_{12}	0.2	0.188	–6.1	0.102	0.103	94.6	0.201	0.4	0.069	0.070	95.6
σ_{22}	1.0	1.016	1.6	0.076	0.076	94.2	1.013	1.3	0.051	0.054	95.8
σ_{11}	1.0	1.008	0.8	0.076	0.076	93.4	1.010	1.0	0.072	0.054	93.4
σ_{12}	0.5	0.492	–1.5	0.090	0.091	95.2	0.497	–0.6	0.088	0.059	93.6
σ_{22}	1.0	1.019	1.9	0.077	0.076	94.6	1.006	0.6	0.052	0.054	95.0
σ_{11}	1.0	1.012	1.2	0.076	0.074	93.6	1.004	0.4	0.056	0.053	93.8
σ_{12}	0.8	0.796	–0.5	0.070	0.067	94.8	0.796	–0.5	0.041	0.039	94.6
σ_{22}	1.0	1.009	0.9	0.074	0.073	94.2	1.007	0.7	0.053	0.053	94.0

[a] Relative bias (%), obtained from the bias divided by the true value.

[b] Empirical standard error; i.e., the standard error of posterior means.

[c] Mean standard error; i.e., the mean of posterior standard deviations.

[d] Coverage probability (%) for 95% credible intervals.

Table 3 The variations and association for event types. σ_{11}: standard deviation of crash, near-crash and CRC; σ_{22}: standard deviation of ULD; ρ_{12}: correlation between the two event types.

	Within-shifts				Between-breaks			
Parameter	Mean	SD[a]	2.5%[b]	97.5%[b]	Mean	SD	2.5%	97.5%
σ_{11}	2.166	0.104	1.974	2.386	2.618	0.220	2.203	3.120
σ_{22}	1.366	0.058	1.256	1.484	1.775	0.146	1.520	2.102

	Within-shifts				Between-breaks			
ρ_{12}	0.888	0.022	0.842	0.930	0.810	0.053	0.697	0.903

[a] Standard deviation of posterior samples.

[b] 2.5% and 97.5% quantiles of posterior samples.